Journal of Applied Polymer Science

Feather-like morphology of poly(methyl methacrylate)/poly(ethylene oxide) blends: The effect of cooling rate and poly(methyl methacrylate) content

Chunyan Luo,[1] Weixing Chen,[1] Ying Gao[2]

[1]Shaanxi Key Laboratory of Photoelectric Functional Materials and Devices, School of Materials and Chemical Engineering, Xi'an Technological University, Xi'an 710021, China

[2]State Key Laboratory of Polymer Physics and Chemistry, Chinese Academy of Sciences, Changchun Institute of Applied Chemistry, Changchun 130022, China

Correspondence to: Y. Gao (E-mail: yinggao@ciac.ac.cn)

ABSTRACT: The effect of cooling rate on the crystallization morphology and growth rate of poly(ethylene oxide) (PEO) and PEO/poly(methyl methacrylate) (PMMA) blends has been observed by Hot Stage Polarized Microscopy (HS-POM). The isothermal crystallization kinetics study was carried out by differential scanning calorimetry (DSC). The spherulite morphology has been observed for the neat PEO with molecular weight of 6000 g/mol. By adding of PMMA with molecular weight of 39,300 g/mol, the growth fronts become irregular. With the increasing of PMMA content, the irregularity of growth front becomes more obvious, and the feather-like morphology can be observed. When PMMA content is 60%, the spherulite is seriously destroyed. This phenomenon is more obvious for the slow cooling process. Based on the measurement of spherulite, the growth rate curves were obtained. According to the curves, it can be seen that the growth rate decreases with the increasing of PMMA content, and the growth rate during the slow cooling process is higher than that of the fast cooling process. The isothermal crystallization experiment indicates that the crystallization rate decreases dramatically with the increasing of PMMA content. And the Avrami parameter n was obtained, which is non-integral and less than 3. Finally, it can be concluded that the higher value of n can be obtained for the condition with low crystallization rate.
 J. Appl. Polym. Sci. **2015**, *132*, 41705.

KEYWORDS: blends; crystallization; morphology

Received 28 June 2014; accepted 30 October 2014
DOI: 10.1002/app.41705

INTRODUCTION

Blending of two polymers can produce special performances and has been widely used in industry. Crystalline materials cover a large portion of polymer family, and the crystallization behavior plays an important role in the condensed structure and property of polymer product. Based on the crystalline or amorphous properties, blends can be divided into three kinds: amorphous/amorphous, crystalline/crystalline, and amorphous/crystalline. Phase separation structures of amorphous/amorphous blends have been investigated by many researchers.[1–8] Many reports also concerned with the crystalline/crystalline[9–11] and amorphous/crystalline[12–15] blends. However, the performance of polymer blends mainly depends on the miscibility of the components. Thus, the blends also can be divided into another three kinds: miscible, immiscible, and partially miscible blends. The miscibility of blends has been widely studied.[16–20] Wu[21] points out that the integrated crystallization behavior occurs in the immiscible systems because of the macrophase separation of blends.

Poly(ethylene oxide) (PEO)/poly(methyl methacrylate) (PMMA) is a partially miscible crystalline/amorphous blend, which has attracted many people's interests.[22–36] In the crystalline/amorphous blend, crystallization and phase separation can occur simultaneously. Pattern formation during crystallization and phase separation in the blends has been studied for a number of years. Okerberg *et al.*[27,28] reported the dendritic crystallization of PEO/PMMA thin films spin-coated from solution on silicon substrate, in which PEO has a weight-average molecular weight of 101,200 and PMMA has a weight-average molecular weight from 4900 to 101,000. In their study, blends with a composition of 50/50 exhibit a variety of morphologies (dendrite, dense-branched morphology, stacked needles, needles) that are highly dependent on PMMA molar mass and crystallization temperature; In 35/65 blends, dendritic growth is observed with

side-branches at 45° and 90° to the dendrite trunk at low undercooling and only at 90° for larger undercooling. Shi *et al.*[31,32] investigated the crystallization pattern formation of PEO/PMMA, in a competing crystallization and phase separation process. In their studies, PEO has a weight-average molecular weight of 20,000 and PMMA has a weight-average molecular weight of 15,000. A morphological inversion from spherulitic to concentric ring patterns by adjusting the quench depth was observed. Wang *et al.*[36] observed the fractal-like branched pattern in in ultrathin PEO/PMMA blend films on glass substrate coated with Au, in which PEO has a weight-average molecular weight of 6000 and PMMA has a weight-average molecular weight of 4200. The presence of PMMA influences strikingly the branch length and thickness by imposing two competitive effects on the PEO crystallization, to accelerate and to retard the crystallization, depending on the film composition. The accelerated crystallization, probably by de-mixing between PEO and PMMA, leads to thinner and longer crystal branches; the retardation effect of PMMA, which results in thicker and shorter crystal branches, is attributed to reducing the mobility of PEO chains in the system.

In the PMMA/PEO blend, PMMA is amorphous and PEO is crystalline. The crystallization of PEO is largely influenced by the miscibility of PMMA and PEO and the PMMA content. Further, the molecular weight plays an important role on the blending structure and chain conformation, i.e., the miscibility, which leads to the change of phase separation structure and crystallization behavior.[37–41] In our previous work,[42,43] the effect of homopolymer molecular weight on the blending structure and crystallization behavior of poly(styrene)-b-poly(ethylene oxide)-b-poly(styrene)/poly(ethylene oxide) (PS-*b*-PEO-*b*-PS/PEO) blends have been investigated.

In most of the above researches, the molecular weights of PMMA are smaller than that of PEO. Shi *et al.*[33] reported the blending system with a larger PMMA molecular weight than PEO, while the content of PMMA is less than 10%. Then how is the crystallization behavior of PEO influenced by PMMA, in which PMMA has a larger molecular weight than PEO and PMMA content more than 10%? In addition, temperature factors, such as annealing temperature, crystallization temperature, quench depth, are concerned in above researches on PEO/PMMA blends. Then how is the cooling rate acting on the crystallization pattern of PMMA/PEO blends? This work will be carried out around the two questions. And the isothermal crystallization kinetics experiment will be carried out to investigate the effect of PMMA on the PEO crystallization behavior in bulk further.

EXPERIMENTAL

Materials

PMMA and PEO were purchased from Shanghai Kumhosunny Plastics Co. and Sinopharm Chemical Reagent Co., respectively. For PMMA, the number-average molecular weight $M_n = 39{,}300$ and $M_w/M_n = 1.97$ where M_w stands for weight-average molecular weight. The molecular weight of PEO is about 6000 as marked on the reagent bottle. The materials were used as received.

Film Preparation. PMMA and PEO were dissolved in dichloromethane with 5% of polymer by weight. The solution was stirred at room temperature over 1 h and let stand for more than 12 h, then casted on a clean glass plate. The solvent was quickly evaporated and further dried under vacuum until constant weight was obtained.

Optical Microscopy. The polarized optical microscopy (POM) was carried out using a Leica optical microscope. The experimental temperature was controlled by a Linkam hot stage. The fast cooling process was carried out by heating to 110°C at 10 °C/min and kept for 3 min, and then naturally cooling down to 10°C under room temperature; the slow cooling process was carried out by heating to 110°C at 10 °C/min and kept for 3 min, and then cooling to 10°C at 1 °C/min.

Differential Scanning Calorimetry. A differential scanning calorimetry (DSC) Q2000-TA was used to characterize the melting and crystallization behavior of the blends. The calibration was carried out with indium and zinc. The heating and cooling scans were performed at the rate of 10 °C/min during the non-isothermal experiments. The isothermal crystallization experiment was carried out by heating sample to 150°C at 20 °C/min, and then ramp to isothermal temperatures for 50 min.

RESULT AND DISCUSSION

Crystallization Morphology of Neat PEO

Figure 1 shows the optical micrograph of a typical spherulitic morphology of neat PEO observed during crystallization by fast (upper row) and slow (lower row) cooling processes. The typical Maltese-cross spherulitic morphology can be observed during both cooling processes. And the growth fronts of spherulite in the two cooling processes are both regular. The difference also exists, i.e., the size of spherulite observed in the slow cooling process is obviously lager than observed in the fast cooling process. The results indicate that the change of cooling rate doesn't influence the spherulitic morphology of neat PEO, while the size of spherulite is larger during the slow cooling crystallization process.

Crystallization Morphology of PMMA/PEO Blends

Figure 2 shows the optical micrograph of spherulitic morphology of PMMA/PEO blend with a PMMA weight fraction of 10% observed during crystallization by fast (upper row) and slow (lower row) cooling processes. For the fast cooling process, the Maltese-cross spherulitic morphology with regular growth front can also be observed. The adding of 10% PMMA doesn't change the spherulitic morphology of PEO much. And due to the same reason, the size of spherulite is larger during the slow cooling process. However, the change occurs during the slow cooling process by adding of 10% PMMA compared to the neat PEO, the growth front is not regular any more. The irregular growth front is not observed during the fast cooling process. For the PMMA/PEO blend with 40% PMMA, the irregular growth front is more obvious as shown in Figure 3. With the increasing of PMMA content, the spherulite of PEO becomes much more irregular, and not so integrated. For the fast cooling process, the bundled lamellar crystal is disordered and the Maltese-cross is not so clear. But for the slow cooling process, the spherulite with clear Maltese-cross and feather-like morphology can be observed. With the further increasing of PMMA content to 60%, the character of spherulite is almost lost (shown in Figure 4). The dark amorphous region appears in the

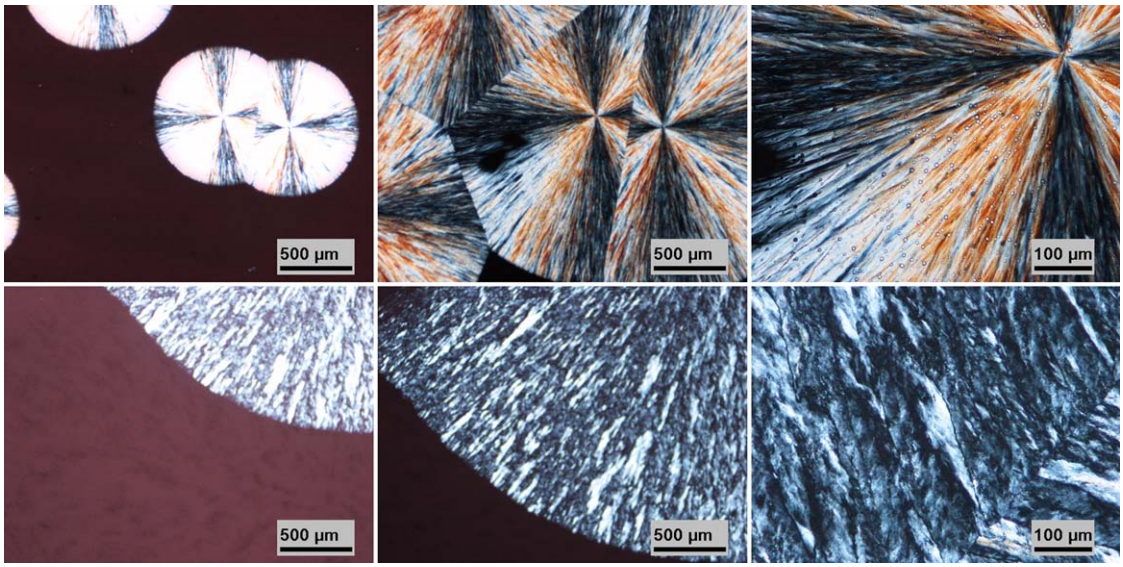

Figure 1. Time evolution of the spherulitic pattern of neat PEO by fast (upper row) and slow (lower row) cooling process under POM. [Color figure can be viewed in the online issue, which is available at wileyonlinelibrary.com.]

crystal structure. And the feather-like structure can be observed in some local areas. The larger size of irregular spherulite and more clearly feather-like structure can be observed during the slow cooling process compared to the fast cooling process.

Above all, several phenomena can be summarized in this work.

Firstly, the size of spherulite is larger during slow cooling process. The change of spherulite size is due to the difference of crystallization temperature. For the fast cooling condition, the temperature reaches a rather low temperature rapidly, which is suitable for the nucleation process. However, the slow cooling process ensures the crystallization behavior occur at higher temperature, which is more suitable for the growth procedure rather than nucleation.

Secondly, the adding of PMMA (39,300 g/mol) leads to the change of PEO (6000 g/mol) spherulitic morphology, i.e., the worse integrality and the feather-like morphology. The viscosity difference between two components is the main reason. The viscosity of PMMA at 110°C is much higher than the viscosity of PEO. The difference of viscosity is at the scale of 10^6, so the PEO melt is moving much faster than PMMA. Further, when the temperature decreases from the melted state, the PMMA chains come into glassy state from high elastic state when the temperature is less than its glassy transition temperature (about 100°C). Then the PMMA chains can move hardly, the phase separation will be obvious. When PMMA content is low, the integrality of PEO spherulite is as good as neat PEO, because most PMMA was ejected from PEO crystal. While the increasing

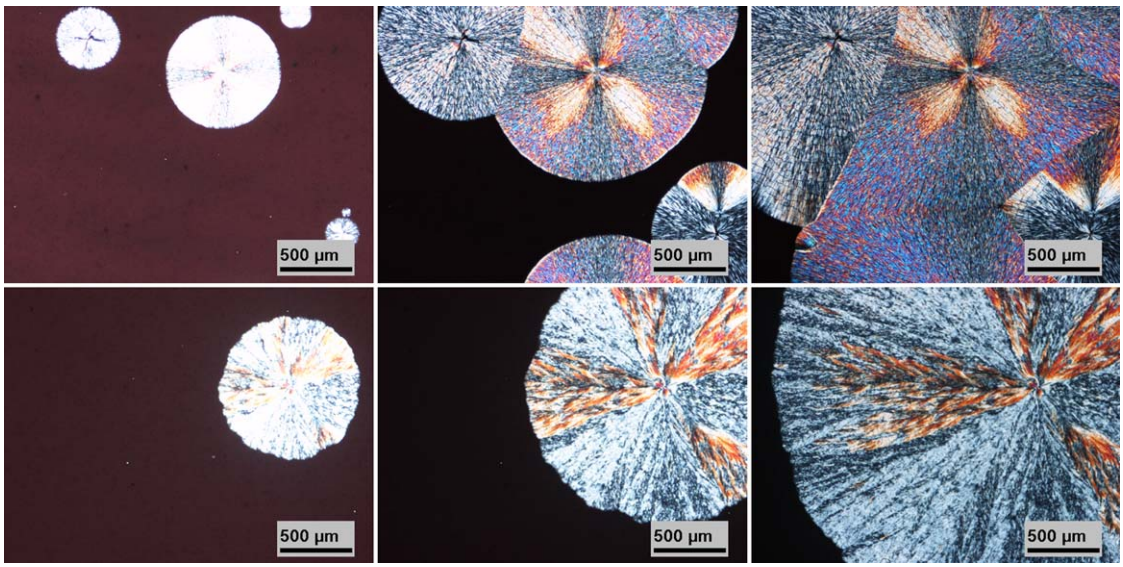

Figure 2. Time evolution of the spherulitic pattern of PEO/PMMA blend (with PMMA weight fraction of 10%) by fast (upper row) and slow (lower row) cooling process under POM. [Color figure can be viewed in the online issue, which is available at wileyonlinelibrary.com.]

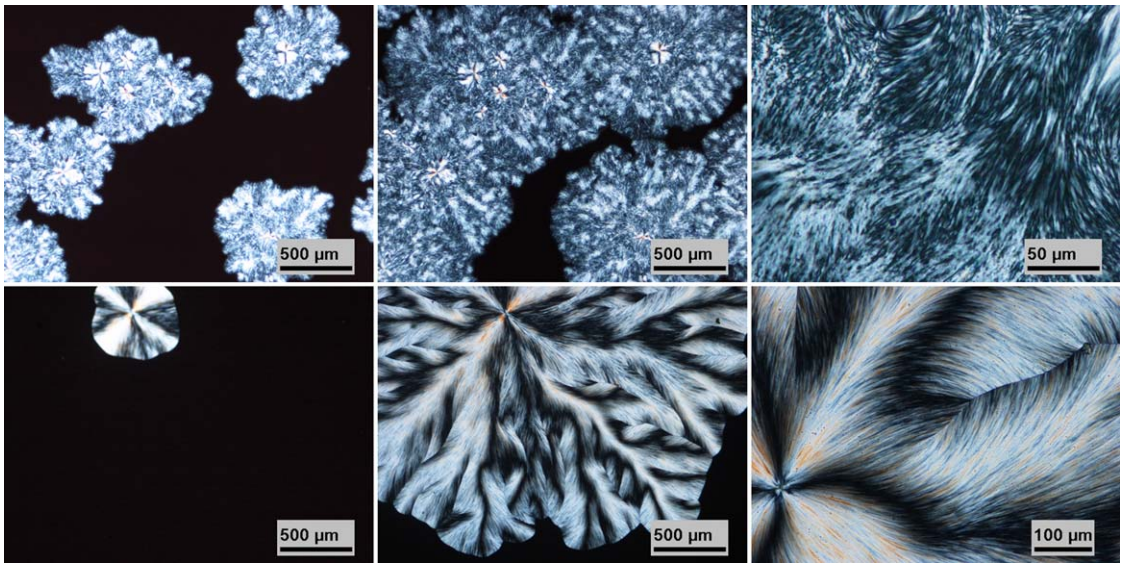

Figure 3. Time evolution of the spherulitic pattern of PEO/PMMA blend (with PMMA weight fraction of 40%) by fast (upper row) and slow (lower row) cooling process under POM. [Color figure can be viewed in the online issue, which is available at wileyonlinelibrary.com.]

of PMMA content causes the formation of irregular growth front, and the images with high magnitude indicates the feather-like morphology, which is very different from the dendrite, dense-branched, stacked needles, needles morphologies for blending systems with smaller molecular weight of PMMA than PEO.[27,28] For the PMMA/PEO blends with larger molecular weight of PMMA than PEO by Shi *et al.*,[33] in which PMMA and PEO have weight-average molecular weights of 100,000 and 24,000 respectively, the spherulitic or concentric ring patterns rather than feather-like morphology are obtained. In their work, when PMMA content was over 10%, they did not observe any crystallization indication in the dynamic calorimetric measurement. However, in our work, the PMMA/PEO blends with much lower PMMA molecular weight crystallize even when the PMMA content is high enough to 60%. The larger the PMMA molecular weight is, the more difficult the PEO crystallizes. Because larger PMMA molecular weight means higher viscosity, which will depress the mobility of PEO chains during cooling crystallization process.

Thirdly, the feather-like morphology is more obvious for the slow cooling process than that of fast cooling process. When the blends are cooled down from the melted state, the phase separation between PEO and PMMA occurs. During the slow cooling process, the viscosity of PEO increases slowly, which provides the phase separation behavior enough time, then the relative flow between PEO and PMMA occurs. The reorganization of PEO molecular into the lamella can expel the PMMA from the

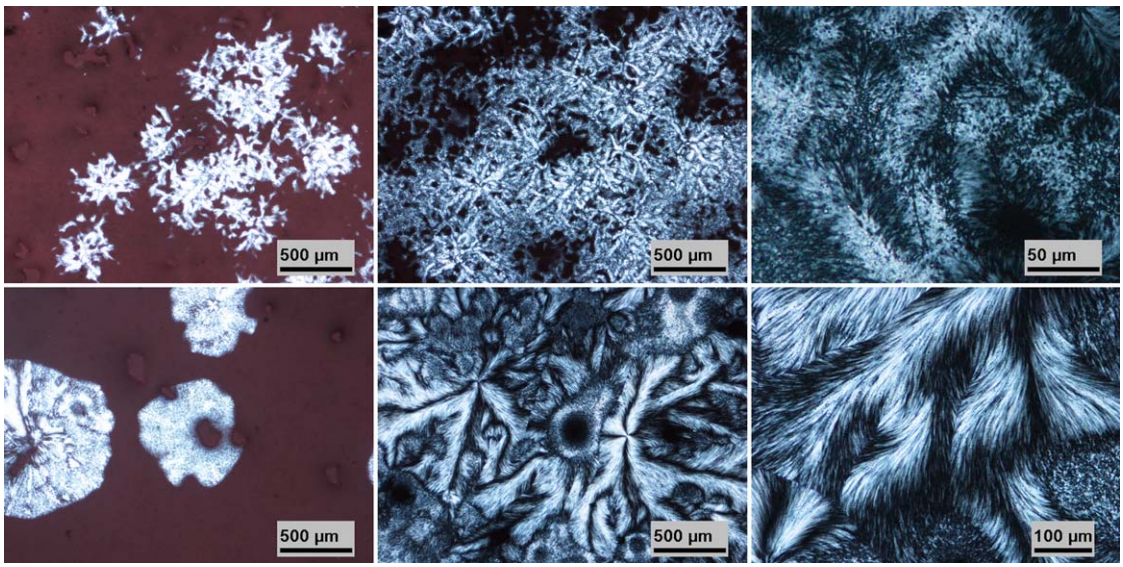

Figure 4. Time evolution of the spherulitic pattern of PEO/PMMA blend (with PMMA weight fraction of 60%) by fast (upper row) and slow (lower row) cooling process under POM. [Color figure can be viewed in the online issue, which is available at wileyonlinelibrary.com.]

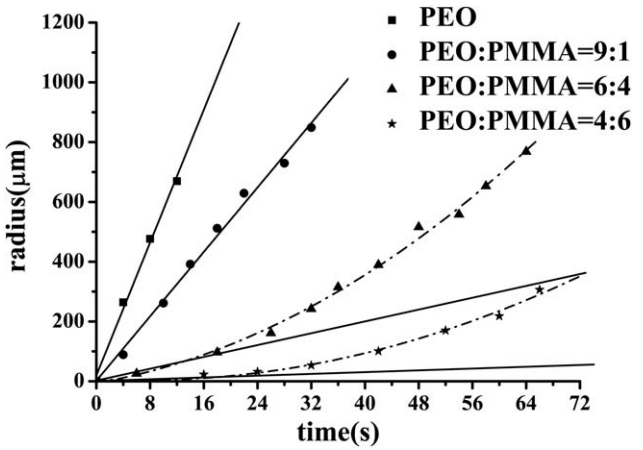

Figure 5. Curves of growth rate for PEO and PEO/PMMA blends (fast cooling).

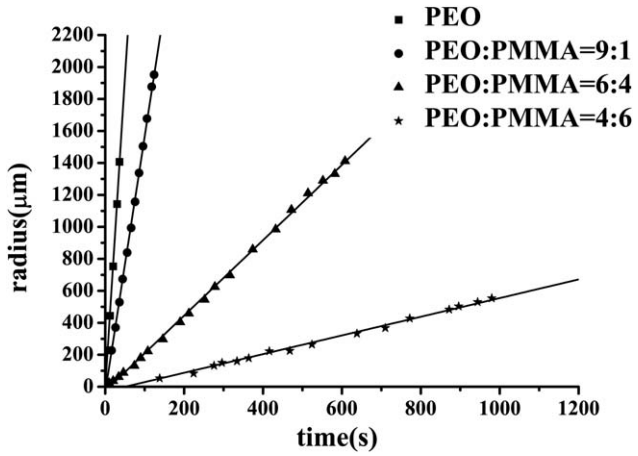

Figure 6. Curves of growth rate for PEO and PEO/PMMA blends (slow cooling).

crystallization structure at low cooling process, which leads to the more clearly feather-like crystallization morphology. However, for the fast cooling process, inadequate time can be provided for the movement of PEO and PMMA chains, the PEO crystal is initiated from multiple nuclei at different positions and the crystallization process is much more localized than slow cooling process.

Growth Rate of Spherulite

The growth rate curves of spherulite for PEO and PEO/PMMA blends during fast and slow cooling processes are shown in Figures 5 and 6, respectively. And the corresponding growth rates are listed in Table I. Compared with neat PEO, the growth rate of PEO/PMMA blends decreases obviously with the increasing of PMMA content both during the fast and the slow cooling processes. And the growth rate during the fast cooling process is higher than that of slow cooling process. Compared with the growth rate curves for slow cooling process, the linear fitting curves for fast cooling process have larger errors, especially for the PEO/PMMA blends with more PMMA, which can even be fitted with multi-times curves presented with dash dot line in Figure 5. The corresponding fitting equations are $y = -5.76 + 3.84x + 0.13x^2$ and $y = 7.32 + 1.09x + 0.08x^2$ for blends with 40% and 60% PMMA, respectively. The decrease of viscosity for blends is slow enough for the spherulite to grow up more perfectly during slow cooling process, which ensures the spherulite growth at a strictly constant speed as shown in Figure 6.

Crystallization Behavior Measured by DSC

In order to analysis the effect of PMMA on the crystallization behavior of PEO further, the crystallization behavior of neat PEO and PEO/PMMA blends in bulk was characterized by DSC. And the corresponding curves are presented in Figure 7. For the neat PEO, the crystallization and melting peak temperatures are at 49°C and 64°C, respectively. With the addition of PMMA, the crystallization peak temperature decreases dramatically, from 49°C to 19°C. However, the decrease of corresponding melting peak temperature is not obvious. According to the crystallization and heating curves, the crystallization peak area and the melting peak area are both decreased, which means that the crystallinity of PEO is depressed by the addition of amorphous PMMA (the crystallization and melting enthalpy is divided by the mass of PEO). When the PMMA content reaches to 60%, no obvious crystallization peak can be observed, and the corresponding melting peak is rather small. It indicates that the crystallization behavior of PEO in the blends is largely restrained by the large amount of amorphous PMMA. The reason is that a large amount of PMMA chains immerge into PEO phase and the PEO chains are separated. When the blends are cooled down from high temperature, the poor mobility of PMMA chains will vastly inhibit the movement of PEO chains, thus the crystallinity of PEO decreases.

In order to investigate the effect of PMMA on the crystallization kinetics of PEO, the nonisothermal crystallization investigation for neat PEO and PEO/PMMA was carried out. The plots of relative crystallinity versus crystallization time at different temperature are presented in Figure 8. The analysis of isothermal crystallization can be carried out by Avrami equation as follows:

$$\lg(-\ln(1-X(t))) = \lg K + n\lg t$$

in which, n is the Avrami parameter, and $\lg K$ is the common logarithm of rate constant by cooling crystallization. The value of n and $\lg K$ can be obtained based on the plots of $\lg(-\ln(1 - X(t)))$ versus $\lg t$ presented in Figure 9. Then the half-time of crystallization $(t_{1/2})$ can be calculated by the following equation:

Table I. Growth Rate of PEO and PEO/PMMA Blends

Composition	PEO	PEO: PMMA = 9: 1	PEO: PMMA = 6: 4	PEO: PMMA = 4: 6
Fast cooling	55.55 μm/s	26.95 μm/s	5.15 μm/s	4.48 μm/s
Slow cooling	38.83 μm/s	16.00 μm/s	2.36 μm/s	0.58 μm/s

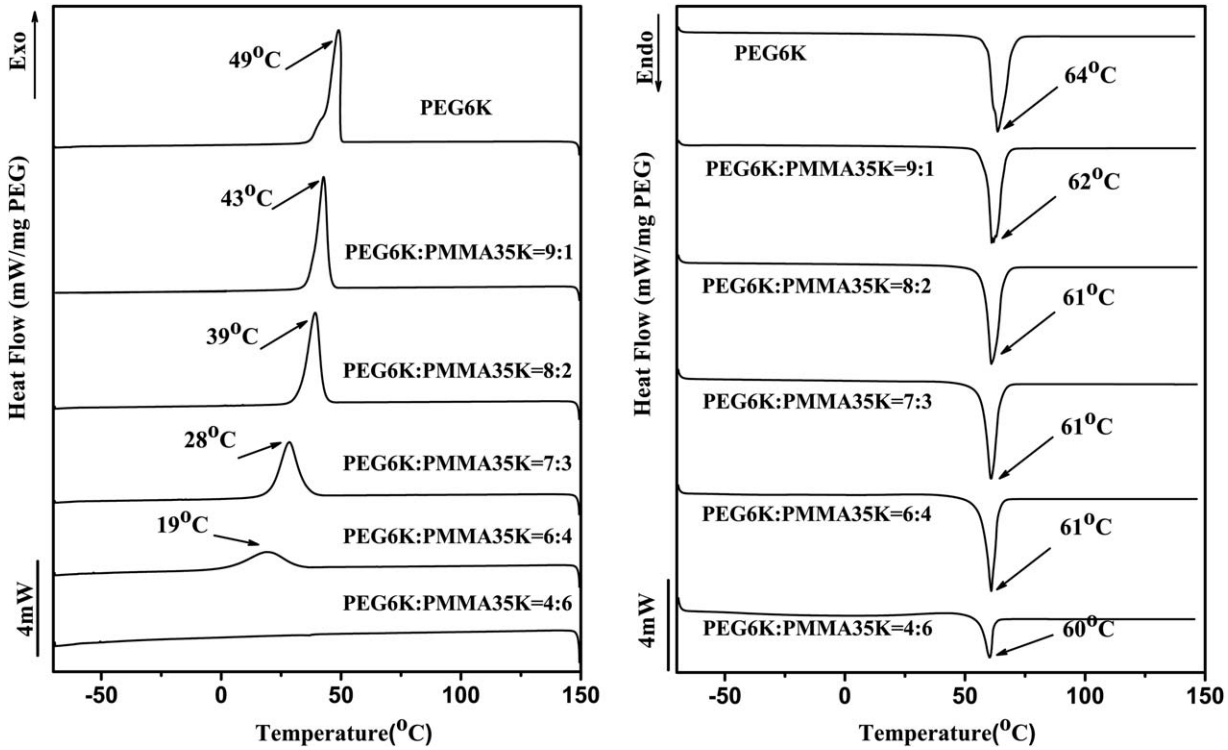

Figure 7. The crystallization curves (Left) and corresponding heating curves (Right) of PEO and PEO/PMMA blends.

$$t_{1/2}=(\ln 2/K)^{1/n}$$

And the reciprocal of $t_{1/2}$ is the crystallization rate (G). The crystallization kinetic parameters at different temperature are presented in Table II.

The fitting curves of $\lg(-\ln(1-X(t)))$ versus $\lg t$ plot exhibit rather good linearity as shown in Figure 9, which indicates that the Avrami equation can be used to analyze the crystallization kinetic behavior of PEO and PEO/PMMA blends. According to the values of several kinetic parameters shown in Table II, it can be seen that the crystallization rate G for neat PEO is larger than that of blends, and the crystallization rate decreases with the increasing of PMMA content at the same temperature. The reason is that when the crystallization behavior occurs, the added PMMA stays at the glassy state, i.e., the PMMA chains can move hardly, which depresses the mobility of PEO chains. Further, the crystallization rate increases with the decreasing of the isothermal crystallization temperature. The decrease of temperature leads to the increasing of nucleation rate, thus the crystallization rate is larger at lower temperature during the experimental temperature range.

The values of n for neat PEO and PEO/PMMA blends at different temperature as presented in Table II are not integers, and the values are lower than the value of spherulite ($n=3$ for

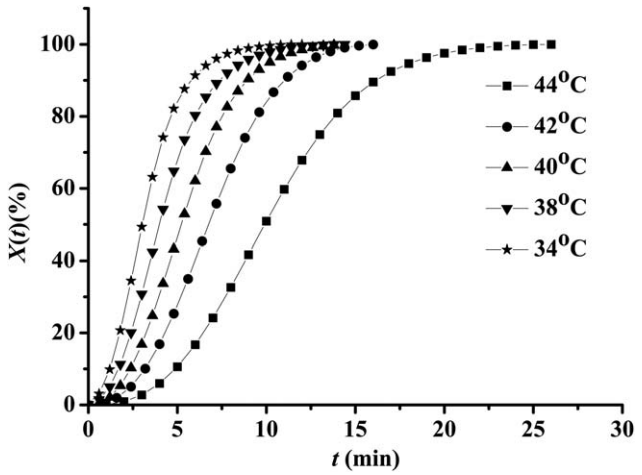

Figure 8. Relative crystallinity versus crystallization time for PEO/PMMA blends (with 40% PMMA).

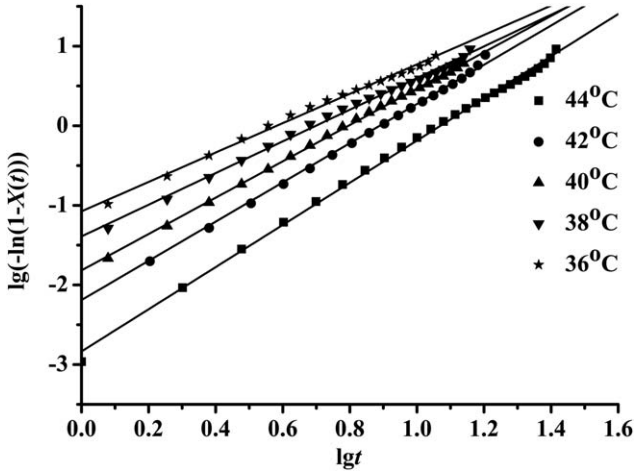

Figure 9. Plot of $\lg(-\ln(1-X(t)))$ versus $\lg t$ for isothermal crystallization of PEO/PMMA blends (with 40% PMMA).

Table II. Crystallization Kinetic Parameters for PEO and PEO/PMMA Blends

	T (°C)	n	lg$K$	$K \times 10^3$	$t_{1/2}$ (min)	G (min^{-1})
Neat PEO	52	2.1	−1.596	25.35	4.808	0.21
	50	1.8	−0.360	436.5	1.288	0.78
	48	1.1	0.036	1086.4	0.676	1.48
PEO: PMMA = 9: 1	50	2.2	−1.785	16.41	5.395	0.19
	48	1.6	−0.754	176.2	2.346	0.43
	46	1.5	−0.292	510.5	1.219	0.82
PEO: PMMA = 8: 2	50	2.0	−1.539	28.91	5.058	0.20
	48	1.8	−0.958	110.2	2.802	0.36
	46	1.7	−0.661	218.3	1.949	0.51
PEO: PMMA = 6: 4	44	2.6	−2.835	1.462	10.24	0.10
	42	2.5	−2.190	6.457	6.671	0.15
	40	2.3	−1.817	15.24	5.319	0.19
	38	2.0	−1.390	40.74	4.154	0.24
	36	1.8	−1.075	84.14	3.134	0.32

heterogeneous nucleation). The values of n, for neat PEO and PEO/PMMA blends with different PMMA content, are larger at higher isothermal crystallization temperature in which the crystallization rate is much lower. For example, the value of n for PEO/PMMA blends with 60% PMMA decreases from 2.6 to 1.8 when the temperature decreases from 44°C to 36°C, and the corresponding crystallization rate G increasing from 0.10 to 0.32. Considering all the systems, the maximum value of n is 2.6 and the corresponding crystallization rate G is as low as 0.10; the minimum value of n is 1.1 and the corresponding crystallization rate G is as high as 1.48. In a word, the larger value of n can be obtained when the crystallization rate is low. The low crystallization rate is obtained from the systems at higher isothermal crystallization temperature or the blends with larger amount of PMMA, in which the larger size of crystal can be obtained, i.e., the crystal will grow more integrated without the collision of other crystals. PEO is a kind of crystalline homopolymer with very large crystallization rate, so the value of n we obtained is non-integral and less than 3. In conclusion, the Avrami parameter n is not very suitable to be used to describe the nucleation and growing mode. But we can use the Avrami equation to obtain the crystallization rate and further analysis the relationship between crystallization rate G and the value of n.

Based on the DSC results, we can know that the addition of PMMA leads to the decrease of crystallization rate of PEO dramatically, and the integrality of the PEO crystals is also destroyed greatly, which is consistent with the POM observation results.

CONCLUSION

The effect of cooling rate on the crystallization morphology and crystallization rate of PEO and the miscible PEO/PMMA blends has been carried out in this work by POM. And the growth rate curves of the PEO and PEO/PMMA blends were obtained by the measurement of spherulitic radii both for the fast and slow cooling processes. The POM images present the spherulite morphology and the feather-like morphology for the PEO and PEO/PMMA blends, respectively, which indicates that the addition of PMMA change the PEO morphology seriously. The POM images for the fast and slow cooling processes indicate that the irregularity of spherulite and the feather-like morphology are much more obvious during the slow cooling process. The growth rate curves indicate that the growth rate of PEO decreases with the increasing of PMMA content and decreases with the decreasing of cooling rate. Based on the crystallization kinetics by DSC study, it can be seen that the slow crystallization rate corresponds to a larger value of n, because the slow crystallization behavior leads to more integrated crystal.

ACKNOWLEDGMENTS

This work was supported by the National Natural Science Foundation of China (Projects No. 21274151), the Principal's Fund of Xi'an Technological University (Projects No. XAGDXJJ1208) and the Opening Fund of Shaanxi Key Laboratory of Photoelectric Functional Material and Instruments (Projects No.ZSKJ201418).

REFERENCES

1. Chen, C.; Maranas, J. K. *Macromolecules* **2009**, *42*, 2795.
2. Chung, H. O.; Ohno, K.; Fukuda, T.; Composto, R. *J. Macromolecules* **2007**, *40*, 384.
3. Li, X.; Han, Y. C.; An, L. *J. Appl. Surf. Sci.* **2004**, *230*, 115.
4. Li, X.; Han, Y. C.; An, L. *J. Polymer* **2003**, *44*, 8155.
5. Ton-That, C.; Shard, A. G.; Daley, R.; Bradley, R. H. *Macromolecules* **2000**, *33*, 8453.
6. Ton-That, C.; Shard, A. G.; Teare, D. O. H.; Bradley, R. H. *Polymer* **2001**, *42*, 1121.
7. Wang, H.; Composto, R. *J. Interface Sci.* **2003**, *11*, 237.
8. Zong, J.; Xie, X. M.; Wang, X. F. *Chem. J. Chin. Univ.* **2004**, *25*, 2363.
9. Ikehara, T.; Kurihara, H.; Qiu, Z.; Nishi, T. *Macromolecules* **2007**, *40*, 8726.
10. Qiu, Z.; Ikehara, T.; Nishi, T. *Polymer* **2003**, *44*, 2799.

11. Qiu, Z. B.; Yan, C. Z.; Lu, J. M.; Yang, W. T.; Ikehara, T.; Nishi, T. *J. Phys. Chem. B* **2007**, *111*, 2783.
12. Basire, C.; Ivanov, D. A. *Phys. Rev. Lett.* **2000**, *85*, 5587.
13. Bouapao, L.; Tsuji, H.; Tashiro, K.; Zhang, J.; Hanesaka, M. *Polymer* **2009**, *50*, 4007.
14. Ling, G. H.; Shaw, M. T. *Polymer* **2009**, *50*, 4917.
15. Pan, P.; Liang, Z.; Zhu, B.; Dong, T.; Inoue, Y. *Macromolecules* **2009**, *42*, 3374.
16. Lee, J. H.; Ruegg, M. L.; Balsara, N. P.; Zhu, Y.; Gido, S. P.; Krishnamoorti, R.; Kim, M. H. *Macromolecules* **2003**, *36*, 6537.
17. Lopez-Barron, C. R.; Macosko, C. W. *Langmuir* **2009**, *25*, 9392.
18. Moon, H. K.; Choi, Y. S.; Lee, J. K.; Ha, C. S.; Lee, W. K.; Gardella, J. A. *Langmuir* **2009**, *25*, 4478.
19. Takeshita, H.; Shiomi, T.; Suzuki, T.; Sato, T.; Miya, M.; Takenaka, K.; Wacharawichanant, S.; Damrongsakkul, S.; Rimdusit, S.; Thongyai, S.; Taepaisitphongse, V. *Polymer* **2005**, *46*, 11463.
20. Tanaka, S.; Nishida, H.; Endo, T. *Macromolecules* **2008**, *42*, 293.
21. Wu, P. X. *J. HEBEI Inst. Technol.* **1994**, *23*, 62.
22. Brodeck, M.; Alvarez, F.; Colmenero, J.; Richter, D. *Macromolecules* **2012**, *45*, 536.
23. Ferreiro, V.; Douglas, J. F.; Amis, E. *J. Macromol. Symp.* **2001**, *167*, 73.
24. Ghelichi, M.; Qazvini, N. T.; Jafari, S. H.; Khonakdar, H. A.; Farajollahi, Y.; Scheffler, C. *J. Appl. Polym. Sci.* **2013**, *129*, 1868.
25. Li, X.; Hsu, S. L. *J. Polym. Sci.: Polym. Phys. Edit.* **1984**, *22*, 1331.
26. Martuscelli, E.; Silvestre, C.; Addonizio, M. L.; Amelino, L. *Makromol. Chem.* **1986**, *181*, 1557.
27. Okerberg, B. C.; Marand, H. *J. Mater. Sci.* **2007**, *42*, 4521.
28. Okerberg, B. C.; Marand, H.; Douglas, J. F. *Polymer* **2008**, *49*, 579.
29. Schwahn, D.; Pipich, V.; Richter, D. *Macromolecules* **2012**, *45*, 2035.
30. Shi, J.; Wang, Y. M. *J. Funct. Polym.* **2003**, *16*, 69.
31. Shi, W.; Cheng, H.; Chen, F.; Liang, Y.; Xie, X.; Han, C. C. *Macromol. Rapid Commun.* **2011**, *32*, 1886.
32. Shi, W.; Han, C. C. *Macromolecules* **2012**, *45*, 336.
33. Shi, W.; Xie, X. M.; Han, C. C. *Macromolecules* **2012**, *45*, 8336.
34. Sterzynski, T.; Garbarczyk, J. *J. Mater. Sci.* **1991**, *26*, 6357.
35. Suvorova, A. I.; Hassanova, A. H.; Tujkova, I. S. *Polym. Int.* **2000**, *49*, 1014.
36. Wang, M.; Braun, H. G.; Meyer, E. *Polymer* **2003**, *44*, 5015.
37. Hashimoto, T.; Koizumi, S.; Hasegawa, H. *Macromolecules* **1992**, *25*, 1433.
38. Hashimoto, T.; Koizumi, S.; Hasegewa, H. *Phys. B* **1995**, *213–214*, 676.
39. Hashimoto, T.; Tanaka, H.; Hasegawa, H. *Macromolecules* **1990**, *23*, 4378.
40. Koizumi, S.; Hasegawa, T. H.; Hashimoto, T. *Macromolecules* **1994**, *27*, 7893.
41. Tanaka, H.; Hasegawa, H.; Hashimoto, T. *Macromolecules* **1991**, *24*, 240.
42. Gao, Y.; Liu, H. L. *J. Appl. Polym. Sci.* **2007**, *106*, 2718.
43. Luo, C. Y.; Han, X.; Gao, Y.; Liu, H. L.; Hu, Y. *J. Appl. Polym. Sci.* **2009**, *113*, 907.